Evolution of the Fermi surface of arsenic through the rhombohedral to simple-cubic phase transition: A Wannier interpolation study

Patricia K. Silas,[1] Peter D. Haynes,[2] and Jonathan R. Yates[3]

[1]*Theory of Condensed Matter, Cavendish Laboratory, University of Cambridge, JJ Thomson Avenue, Cambridge CB3 0HE, United Kingdom*

[2]*Departments of Materials and Physics, Imperial College London, Exhibition Road, London SW7 2AZ, United Kingdom*

[3]*Department of Materials, University of Oxford, Parks Road, Oxford OX1 3PH, United Kingdom*

(Received 14 August 2012; revised manuscript received 28 June 2013; published 9 October 2013; publisher error corrected 15 October 2013)

The pressure dependence of the Fermi surface of arsenic is examined using the technique of Wannier interpolation, enabling a dense sampling of the Brillouin zone and the ability to capture fine features within it. Focusing primarily on the A7 → simple-cubic phase transition, we find that this semimetal to metal transition is accompanied by the folding of Fermi surfaces. The pressure dependence of the density of states (DOS) of arsenic indicates that the onset of the Peierls-type cubic to rhombohedral distortion is signified by the appearance of emerging van Hove singularities in the DOS, especially around the Fermi level. As we noted in an earlier study, high levels of convergence are consequently required for an accurate description of this transition.

DOI: 10.1103/PhysRevB.88.134103 PACS number(s): 61.50.Ks, 61.66.Bi, 71.18.+y, 71.20.−b

I. INTRODUCTION

At ambient pressures the group-V element arsenic is a semimetal with the rhombohedral α-As or A7 crystal structure (space group $R\bar{3}m$). Under applied pressure arsenic undergoes a series of structural phase transitions,[1] the first of which occurs at approximately 28 GPa yielding the metallic simple-cubic (sc) structure (space group $Pm\bar{3}m$). The change in the electronic structure of arsenic across this semimetal to metal phase transition is described most naturally using the Fermi surface. In the A7 phase, arsenic is known to have a very unusual Fermi surface, consisting of six lobes connected by six long thin cylinders or "necks." This Fermi surface is today still depicted as it was by Lin and Falicov[2] in 1966—an artist's rendition—it is a famous image that is often used to describe the complexity that a Fermi surface may exhibit. First-principles calculations on the very dense grids required to resolve the fine details of the Fermi surface of arsenic are computationally expensive even with contemporary computing resources. Here we demonstrate that the method of Wannier interpolation[3–6] achieves the same accuracy far more inexpensively.

In this study we use Wannier interpolation to investigate the pressure dependence of the Fermi surface and density of states (DOS) of arsenic, in particular as it experiences the A7 → sc semimetal to metal phase transition. Wannier interpolation of the band structure is based on the use of maximally localized Wannier functions (MLWFs),[7–9] which act in the spirit of "tight-binding" as a set of spatially-localized orbitals, allowing calculations to be performed with the accuracy of first-principles simulations but at low computational cost. Indeed, arsenic provides us with a beautifully simple demonstration of the power of Wannier interpolation—it is an ideal testing ground for the use of this technique to study phase transitions involving a metal.

In an earlier work we used density-functional theory (DFT) to determine the transition pressure of the A7 → sc phase transition of arsenic.[10] The investigation consisted of performing relaxations of the two-atom unit cell subjected to pressures over the range of 0–200 GPa. The study was focused primarily on the A7 → sc semimetal to metal phase transition. That work enabled us to address a long-standing question as to whether experimental results for the transition pressure obtained by Beister *et al.*[11] were correct over those of Kikegawa and Iwasaki,[12] with our results supporting the findings of the former. It further allowed us to explain the wide range of theoretical values for the transition pressure that can be found in the literature—the spread of values is due to the difficulty of adequately sampling the Brillouin zone (BZ). We discovered that high-quality results required extensive convergence testing with respect to BZ sampling and amount of smearing used. In particular, we found that in order to ensure convergence and reliability of results when studying phase transitions involving a metal, dense BZ sampling grids are essential.[13]

We thus begin by using Wannier interpolation to determine the Fermi surface of arsenic at 0 GPa. We inspect closely the finest features of the electron and hole Fermi surfaces at ambient pressures and make a quantitative comparison of our results with those available in the literature. Building on the results obtained from the relaxations performed in our earlier study,[10] we then use Wannier interpolation to investigate the pressure dependence of the Fermi surface of arsenic, and in particular to study exactly how it evolves through the A7 → sc transition. Finally, we use Wannier interpolation to investigate the DOS of arsenic over a range of different pressures. In our earlier study, we found that converging our geometry optimizations in the vicinity of the A7 → sc phase transition was rather more difficult than expected.[10,13] We will see that this is due to the rapid change of the DOS around the Fermi level across the transition. Consequently, high levels of convergence are required in order to calculate the transition pressure accurately.

The paper is organized as follows. Section II outlines important technical aspects of the methodology, and Sec. III deals with the computational details of our calculations. In Secs. IV to VII, we present and discuss our results: we reveal the actual Fermi surface of uncompressed arsenic—the features thereof are compared to results of theory and experiment that exist in the literature; we study the pressure

dependence of the Fermi surface of arsenic, with a view to observing it as it undergoes the A7 → sc structural phase transition; we calculate the Wannier-interpolated DOS of arsenic in the A7 and sc phases, and we present the pressure dependence of the DOS of arsenic in the immediate vicinity of the A7 → sc transition; we conclude with a brief discussion.

II. METHODOLOGY

A. Wannier interpolation

A conventional electronic-structure calculation yields a set of Bloch states describing the low-lying band structure of a particular system in its ground state. A set of (generalized) Wannier functions[14] (WFs) can be constructed from these Bloch states in order to be able to describe the system in real space, with the WFs acting as a basis set of localized orbitals. The method of Wannier interpolation[3–6] is based on the use of a *unique* set of Wannier functions, the so-called "maximally localized Wannier functions",[7–9] which serve as an "exact tight-binding" basis for the target system. Prescriptions due to Marzari and Vanderbilt[7] and Souza *et al.*[8] allow the determination of this unique set of Wannier functions—the former in the case of a set of isolated bands and the latter extended to the case of a set of entangled bands—by requiring the resulting WFs to exhibit minimum spread.

Wannier interpolation is a simple and widely applicable scheme that incorporates the idea of a tight-binding model with the accuracy of *ab initio* methods. The technique is ideal for the evaluation of quantities that require a very dense sampling of the BZ. In particular, it should be very useful for the study of metallic systems as it enables a sampling of the Fermi surface to *ab initio* accuracy but with little associated cost.

Here we are concerned with finding the eigenvalues of the one-electron effective Hamiltonian at arbitrary $\mathbf{k}$, $\varepsilon_{n\mathbf{k}}$, where n is the band index. However, this interpolation procedure can be extended to the calculation of other quantities of interest—the eigenvalues of any periodic one-electron operator can be determined in a similar fashion.[3]

B. Adaptive smearing

To accelerate the convergence of singularities in the DOS, we apply a state-dependent broadening scheme as follows. Within the Wannier interpolation method, we have the ability to vary the smearing of the occupancies according to the band gradients $|\partial\varepsilon_{n\mathbf{k}}/\partial\mathbf{k}|$, as the gradients can be computed efficiently at no additional cost. The state-dependent smearing width $W_{n\mathbf{k}}$ is set to[3]

$$W_{n\mathbf{k}} = a \left| \frac{\partial \varepsilon_{n\mathbf{k}}}{\partial \mathbf{k}} \right| \Delta k, \tag{1}$$

where a is a dimensionless constant, of value 0.2 in this study. This state-dependent broadening scheme is termed "adaptive smearing,"[3] and it enables highly resolved DOSs, especially when combined with the method of cold smearing.[15]

III. COMPUTATIONAL DETAILS

We build on the findings of our earlier studies of arsenic,[10] in which structural relaxations were performed on the two-atom rhombohedral unit cell subjected to a range of pressures. These geometry optimizations resulted in a series of pressure-dependent configurations, characterized by the lattice parameters which are described in the discussion of the unit cell of arsenic found in the Supplemental Material that accompanies this paper.[16] For each configuration (each pressure), we repeat exactly the same procedure.

The computational details are as follows. For each pressure investigated, we first obtain the Bloch states self-consistently using the density-functional-based PWSCF code[17] in the local-density approximation (LDA). We use a scalar-relativistic, norm-conserving pseudopotential generated using the "atomic" code (by Dal Corso, supplied with the QUANTUM ESPRESSO distribution[17]) to describe the core-valence interaction of arsenic. The pseudopotential core radii are as follows: 1.16 Å for the $4s$ and $4p$ states, and 1.22 Å for the $4d$ states, anticipating that we will need to allow for d states at higher pressures.

We perform the self-consistent calculation on our two-atom unit cell of arsenic using a $25 \times 25 \times 25$ Monkhorst-Pack grid, which includes the Γ point. A kinetic energy cutoff of 750 eV is used for the plane-wave expansion of the valence wave functions. A convergence threshold of 1.4×10^{-8} eV is set for the minimization of the total energy, and a cold smearing[15] of 0.27 eV is used.

Once the ground state charge density of the system has been determined, using the PWSCF code we then perform a non-self-consistent calculation in order to obtain a reference (*ab initio*) band structure against which the Wannier-interpolated band structure can be compared.

To calculate the WFs, the self-consistent potential is frozen and a non-self-consistent calculation is performed in order to discretize the Bloch states over a uniform mesh of $8 \times 8 \times 8$ $\mathbf{q}$ points. The strong localization of the MLWFs in real space, in addition to the generally accepted exponential fall-off of the WFs, ensures that a grid of this size is sufficient for our needs.[3] (In this paper we adopt the convention used in Ref. 3 of using the symbol $\mathbf{q}$ to denote grid points that belong to the mesh upon which the Bloch states have been stored. This is in order to distinguish these specific $\mathbf{q}$ points from arbitrary sites, labeled $\mathbf{k}$ points, at which the values are obtained through interpolation.) The Bloch states are thus stored on a relatively coarse *ab initio* grid. We have determined that we must use nine WFs per atom of the unit cell in order to ensure that we can capture the character of the bands at higher pressures—this point is elaborated upon in the Supplemental Material.[16] Thus we must construct 18 WFs and with this in mind, we calculate the first 30 bands at each $\mathbf{q}$ point. The 18 WFs can then be constructed from these 30 bands according to the disentanglement procedure prescribed by Souza *et al.*[8] This is performed using the WANNIER90 code.[18]

We obtain highly converged DOSs across the range of pressures studied using a $400 \times 400 \times 400$ interpolation ($\mathbf{k}$ point) mesh.

Although we use the PWSCF code in the LDA, the configurations (the lattice parameters defining the structure of arsenic at each pressure) used in this study were obtained from calculations using the Perdew-Burke-Ernzerhof generalized gradient approximation[19] (abbreviated here as GGA-PBE) for

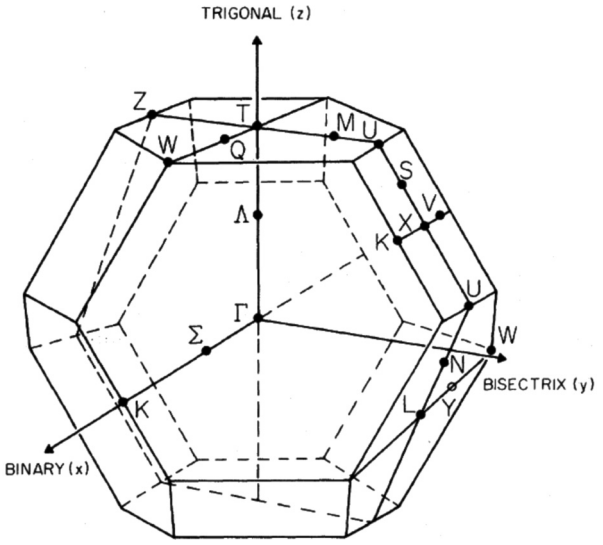

FIG. 1. The BZ of the primitive rhombohedral (A7) structure, labeled with points and lines of symmetry[21,22] and with the mutually orthogonal binary (x), bisectrix (y), and trigonal (z) axes. This figure is taken from Ref. 20. The point along the TW line close to T is labeled as Q in this figure—this point is usually called "B" in the literature and we refer to it throughout this work as B. The special points appearing in the figure are defined explicitly in the Supplemental Material.[16]

the exchange-correlation functional.[10] We have confirmed that when using Wannier interpolation to study the GGA-PBE configurations, it makes no significant difference whether the ground state potential has been set up using an LDA functional or a GGA functional.

IV. THE FERMI SURFACE OF ARSENIC

At 0 GPa, when it is in the A7 phase, arsenic is a semimetal. Only the fifth and sixth bands cross the Fermi level giving rise to the hole and electron Fermi surfaces, respectively. The BZ of the primitive rhombohedral (A7) structure of arsenic is presented in Fig. 1. This figure was taken from Ref. 20, though it was originally published by Cohen in 1961,[21] and it is the same for arsenic as it is for the other group-V semimetals, antimony and bismuth. The special points of the rhombohedral BZ indicated in Fig. 1 have been written out explicitly by Falicov and Golin,[22] and are given in the Supplemental Material that accompanies this work.[16]

The hole Fermi surface, or hole "crown," of arsenic depicted in Fig. 2 was determined by Lin and Falicov via an empirically-based pseudopotential band structure calculation in 1966.[2] It is an artist's rendition, and it is still used today to illustrate the Fermi surface of arsenic.

We use Wannier interpolation to calculate the Fermi surface of arsenic (at 0 GPa) for the first time since Lin and Falicov's calculation. From our $8 \times 8 \times 8$ *ab initio* grid, we interpolate onto a $150 \times 150 \times 150$ $\mathbf{k}$ point grid spanning the BZ in an effort to capture the finest details of the Fermi surface. Given the results of this interpolation and the Fermi energy computed in the initial self-consistent calculation, the Fermi surface is plotted.

The hole Fermi surface of arsenic at 0 GPa resulting from our Wannier interpolation is depicted in Fig. 3—this is as it appears in the reciprocal unit cell. This Fermi surface does closely resemble Lin and Falicov's hole crown. We will investigate how closely further below.

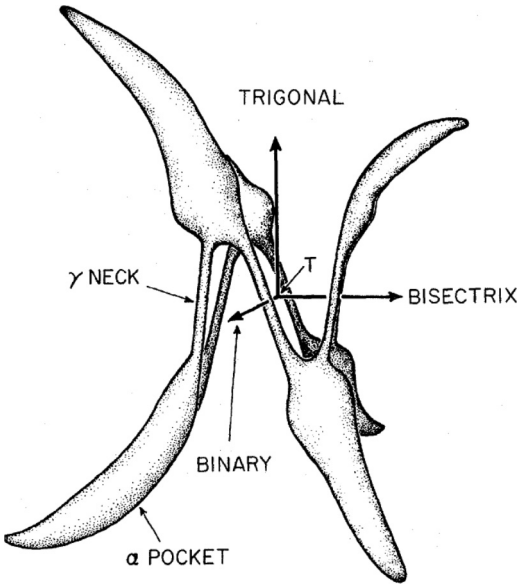

FIG. 2. Lin and Falicov's (Ref. 2) hole crown, taken from Ref. 20. The hole Fermi surface is centered at T. The mutually orthogonal binary (x), bisectrix (y), and trigonal (z) axes are included.

The hole Fermi surface, centered at the point T, is composed of six lobelike pockets connected by six long thin cylinders or necks, each of which is due to a point B of accidental degeneracy located along the TW line and only slightly above the Fermi level. (This accidental degeneracy is believed to be lifted when the spin-orbit coupling is taken into account.[2,24]) The lobes are each bisected by a plane containing the trigonal (ΓT) and bisectrix (ΓU) axes (by a mirror plane). The maximum of the fifth band occurs within the lobe and on the mirror plane at a point designated as "H."

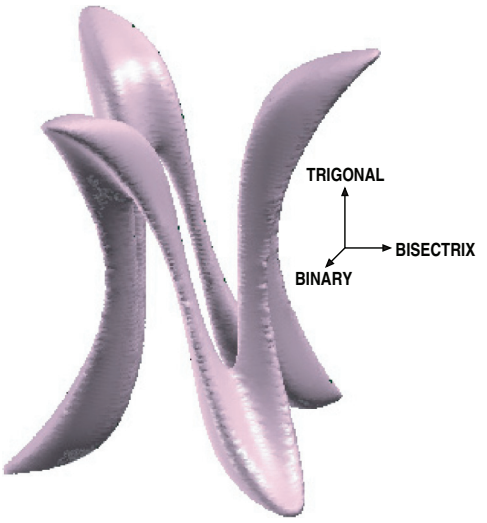

FIG. 3. (Color online) The hole crown of arsenic at 0 GPa as it appears in the reciprocal unit cell. The mutually orthogonal binary, bisectrix, and trigonal axes are included. This has been plotted using the XCRYSDEN package.[23]

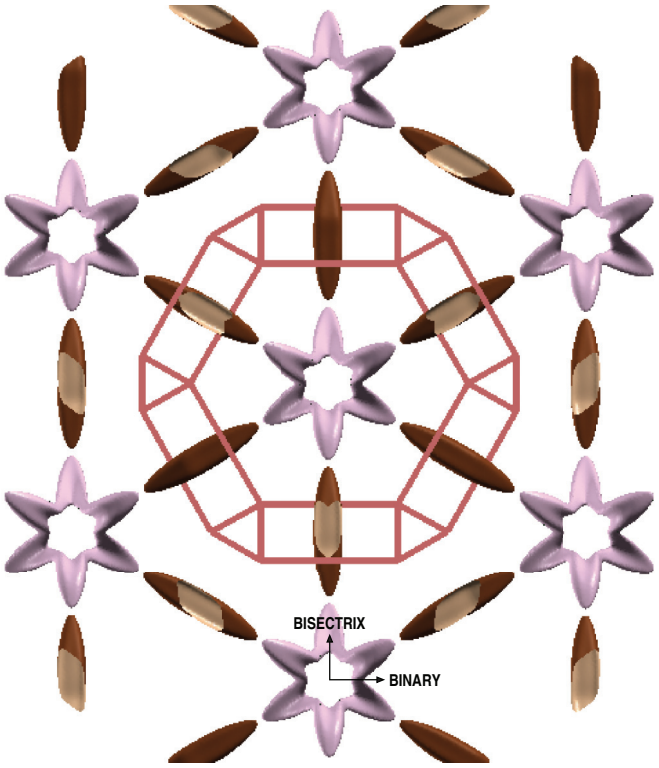

FIG. 4. (Color online) The uncropped hole and electron Fermi surfaces of arsenic at 0 GPa, where the first BZ is displayed. The hole Fermi surface (in light gray/pink) is centered at the point T. Three of the six lobes shown are up, three down. The electron Fermi surface (in dark gray/brown) is comprised of three ellipsoidlike pockets centered at the three equivalent L points of the BZ. The bisectrix axis (TU) is along the vertical, the binary axis (TW) along the horizontal. The trigonal axis is through the origin and out of the page.

The electron Fermi surface is composed of three ellipsoidlike pockets centered at each of the three equivalent L points of the BZ (minimum of the sixth band occurring at L). The merged hole and electron Fermi surfaces of arsenic at 0 GPa are shown in Fig. 4, where the binary (TW) axis lies along the horizontal and the bisectrix (TU) axis lies along the vertical (see Figs. 1 and 2).

We will now go into more detail by looking at certain cross sections of interest of the hole and electron Fermi surfaces of arsenic at 0 GPa, and by comparing our results with those that are available in the literature. This will require interpolating onto two-dimensional grids—slices through the BZ. The Fermi contours resulting from the intersection of these slices with the Fermi surface are subsequently plotted and examined.

We reveal next the intersection of one of these slices through the BZ with the hole Fermi surface, resulting in the contour displayed in Fig. 5. Here we have sliced the hole Fermi surface parallel to the trigonal-bisectrix plane and passing through B. We include as an inset of this figure the equivalent contour obtained by Lin and Falicov in 1966.[2] Our Fermi contour is considerably more detailed than that of Lin and Falicov. The contours resulting from the other slices we inspected are presented in the Supplemental Material,[16] but all results are summarized in Table I and contrasted against data previously published in the literature.

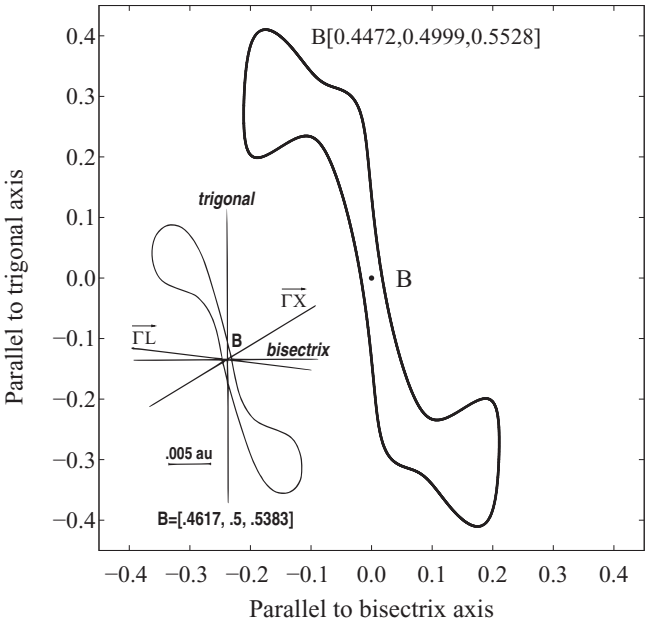

FIG. 5. Hole pocket: trigonal-bisectrix plane through B. This figure has been obtained using a Fermi energy recomputed from the Wannier-interpolated DOS of A7 arsenic at 0 GPa, presented in Sec. VI. All distances are in $Å^{-1}$. The inset is the analogous cross section as calculated by Lin and Falicov.[2]

V. PRESSURE DEPENDENCE OF THE FERMI SURFACE OF ARSENIC: THE A7 → sc PHASE TRANSITION

We illustrate in Fig. 6 the evolution of the electron and hole Fermi surfaces[28] of arsenic as it undergoes the A7 → sc phase transition. This figure is complemented by the corresponding animations 1–3 of the Supplemental Material provided.[16] These animations show the phase transition happening over a finer resolution of pressures than is shown in Fig. 6, and thus give a better idea of what happens to the Fermi surface through the transition.

Figure 6 consists of three columns, each representing a different cross section of the BZ. The four rows of the figure refer to four different pressures: 0, 10, 20, and 35 GPa. In all three columns, the bisectrix axis lies along the horizontal. For the left-hand column the trigonal axis lies along the vertical, whereas for the other two columns the binary axis lies along the vertical. Arsenic is in the A7 phase for the first three rows—it is in the sc phase in the fourth row. Hole surface contours are in black and electron surface contours are in gray (green).

This investigation complements our earlier studies of the A7 → sc phase transition of arsenic.[10] The configurations resulting from geometry optimizations performed on arsenic subjected to pressures up to 200 GPa in that work act as the starting point here for our studies of arsenic using Wannier interpolation. We present our findings concerning the higher-pressure phase transitions of arsenic in the Supplemental Material provided.[16] We expect the A7 → sc phase transition to occur at 28 ± 1 GPa.

We first discuss the left-hand column of Fig. 6, in which the A7 → sc phase transition is most noticeable. The left-hand

TABLE I. Features of the electron and hole Fermi surfaces of arsenic.

Electron Fermi surface. All areas are in $Å^{-2}$	Ref. 2 (theory)	Ref. 25 (experiment)	Ref. 20 (experiment)	This work[a]
Area normal to the binary [see Fig. S3[b]]: trigonal-bisectrix plane through L	0.0571[c]	0.0732 ± 0.0002	0.0733	0.088
Tilt angle[d]	$-8°$	$-9.0 \pm 0.2°$		$-10.6°$
Area normal to the trigonal [see Fig. S4]: binary-bisectrix plane through L	0.0643	0.0746 ± 0.0002	0.0746	0.096
Area normal to the bisectrix [see Fig. S5]: trigonal-binary plane through L			0.0202	0.026
Hole Fermi surface. All areas are in $Å^{-2}$				
Area normal to the binary [see Fig. S6]: trigonal-bisectrix plane through Γ	0.0343	0.01422 ± 0.00002	0.0275	0.027
Tilt angle	$\sim+44°$	$+37.25 \pm 0.1°$	$+37.3 \pm 1.5°$	$+37.8°$
Area normal to the trigonal [see Fig. S7]: binary-bisectrix plane through T	(2.464×10^{-4})[e]	$(2.453 \pm 0.007) \times 10^{-4}$	0.0179	2.1×10^{-3}
Tilt of necks [see Fig. 5]	$-11°$	$-9.6 \pm 0.1°$		$\sim-9.7°$
Combined area normal to the bisectrix [see Fig. S8]: trig.-bin. plane through T			0.0367	0.030
Special $\mathbf{k}$ points H and B. Coordinates are fractional with respect to the reciprocal lattice vectors.	**Ref. 2**	**This work**		
1 of 6 equivalent H points—maximum of the 5^{th} band (occurs in mirror plane)	[0.2043, 0.3758, 0.2043]	[0.2050, 0.3753, 0.2050]		
1 of 6 equivalent B points—point of accidental degeneracy along a TW line	[0.4617, 0.5, 0.5383]	[0.4472, 0.4999, 0.5528]		

[a]These values have been obtained using a Fermi energy recomputed from the Wannier-interpolated DOS of A7 arsenic at 0 GPa, presented in Sec. VI.
[b]Figures for which the numbering begins with an "S" are found in the Supplemental Material (Ref. 16) provided.
[c]Electron pockets: Fermi energy fixed so as to fit the minimum area for magnetic fields in the trigonal-bisectrix plane.
[d]Angle convention followed throughout is that of Ref. 20 (see also Refs. 24–27): angles are measured in the trigonal-bisectrix plane or some parallel plane and with respect to the vertical—the trigonal axis (ΓT) or some parallel line. Positive rotations are in the sense from ΓT to ΓX in the first quadrant of the coordinate system.
[e]Hole pockets: Fermi energy fixed so as to fit this area.

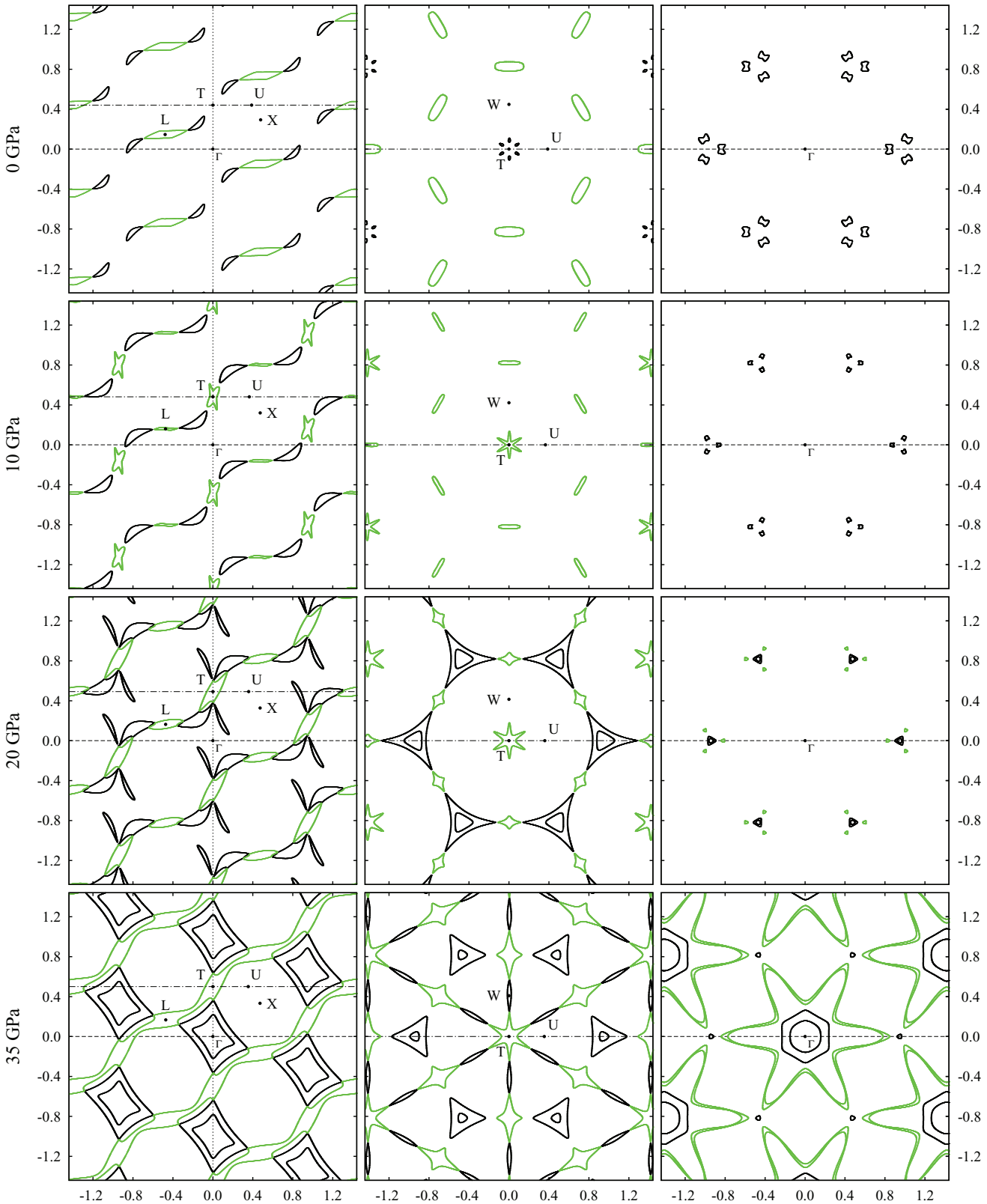

FIG. 6. (Color online) Pressure dependence of the Fermi surface of arsenic: 0–35 GPa. For the left-hand column, the BZ has been intersected by the trigonal-bisectrix plane; the middle column by the binary-bisectrix plane through T; the right-hand column by the binary-bisectrix plane through Γ. The bisectrix axis is along the horizontal for all three columns. The trigonal axis (the finely dotted line) is along the vertical for the left-hand column. The binary axis is along the vertical for the middle and right-hand columns. All distances are fractional with respect to the length of the reciprocal lattice vector—this is to enable comparisons across pressures. Hole contours are in black, electron contours in gray (green). The cross section of the hole crown centered at T can be seen in the top left panel. The A7 → sc phase transition takes place at a pressure between those represented in the bottom two rows of the figure. In the bottom row (at 35 GPa) arsenic is simple cubic—the use of a two-atom unit cell causes the folding evidenced especially in the bottom left and bottom right panels.

column of Fig. 6 corresponds to the intersection of the BZ with the trigonal-bisectrix plane through Γ (it is a mirror plane and contains the points Γ, T, L, X, and U as indicated in the figure). The trigonal axis is the finely dotted vertical line. The other two lines in the diagrams on the left serve to compare orientations with the other two columns.

As we scan from top to bottom in this first column (corresponding to animation 1), we see that the hole surface initially centered on T distorts in such a way that by the bottom panel there is a folded cubic surface (cut along the body diagonal) centered at Γ. Arsenic at 35 GPa is in the sc phase. The surface is folded due to the fact that we have two atoms in the unit cell. We notice too that by 10 GPa an electron pocket has opened up at T (it has actually already opened up by 8 GPa). Our Fermi surfaces fold from about 27 GPa, agreeing with our expected transition pressure of 28 ± 1 GPa.

For the middle column of Fig. 6 (corresponding to animation 2), the BZ has been sliced by the binary-bisectrix plane through T. This slice thus also contains points W and U as indicated. The dotted-dashed line in these figures is the bisectrix axis—as a visual aid for orientation purposes, the bisectrix axis can be compared for corresponding panels of the left-hand and middle columns. The phase transition, again from about 27 GPa, seems to happen when the hole pockets that have opened up at W are just touching the electron pockets appearing on either side of them.

In the right-hand column of Fig. 6 (corresponding to animation 3), the BZ has been sliced by the binary-bisectrix plane through Γ. The dashed lines appearing in the panels of this column correspond to the dashed lines appearing in the panels of the left-hand column of the figure. At about 27 GPa, we once again see the folding of the individual electron and hole Fermi surfaces indicating that arsenic is now in the sc phase.

We have mentioned that the folding of the Fermi surfaces seen in the bottom row of Fig. 6 is due to the fact that we are using the two-atom unit cell to model arsenic over the entire range of pressures studied, whereas in the sc phase the primitive cell contains one atom. The *unfolded* Fermi surfaces can be inspected by comparing the bottom row of Fig. 6 with Fig. S9 of the Supplemental Material,[16] in which are presented the corresponding results for sc arsenic at 35 GPa using a one-atom primitive cell. The BZ for the one-atom primitive sc structure can be found, for example, in Ref. 29 or more recently in Ref. 30.

Determining the pressure at which the A7 → sc transformation of arsenic happens is difficult due to the nature of this semimetal to metal phase transition, which in our earlier study we found to be of second order.[10] In that work, we investigated the pressure dependence of the lattice parameters of arsenic, and we determined the transition pressure according to when the internal coordinates had reached their high-symmetry values. However as the internal coordinates reached their high-symmetry values at two different pressures, there was still some question as to when the transition actually happens. Using Wannier interpolation we have observed the evolution of certain cross sections of interest of the Fermi surfaces across the transition. Wannier interpolation allows us to say that the folding of the Fermi surfaces is perhaps the best indication of when the A7 → sc phase transition has occurred.

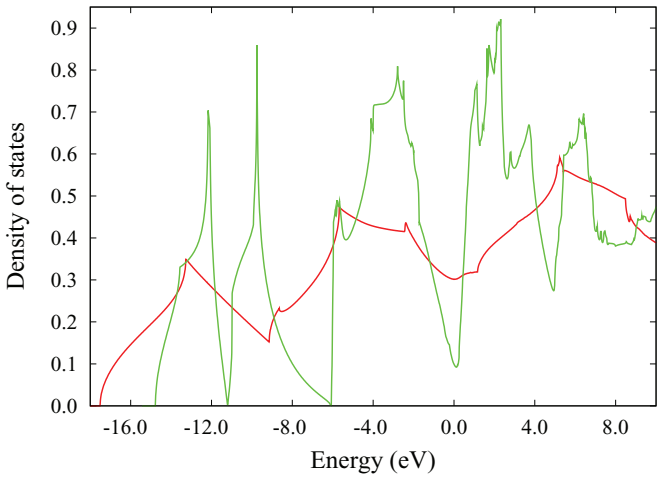

FIG. 7. (Color online) Wannier interpolation combined with adaptive smearing (Ref. 3) using cold smearing (Ref. 15): comparing the DOSs of A7 and sc arsenic—the pressures are 0 (gray/green) and 35 GPa (black/red), respectively. The DOSs are referenced to the Fermi level in both cases. This figure can be compared to that which appears in Ref. 31. Our results agree qualitatively with those. It is evident that Wannier interpolation combined with adaptive smearing enables features of the DOS to be captured on the very finest of scales. The DOS at the Fermi level can be seen to increase appreciably through the A7→sc transition, as arsenic changes from a semimetal to a metal.

VI. WANNIER-INTERPOLATED DENSITIES OF STATES OF A7 AND sc ARSENIC

Wannier-interpolated DOSs for arsenic in the A7 phase at 0 GPa and in the sc phase at 35 GPa obtained using the WANNIER90 code[18] are presented in Fig. 7. This figure can be compared with that which appears in Ref. 31. Our results agree at least qualitatively with those (the pressures corresponding to the DOSs in that publication are not specified), the only other DOS calculations of arsenic of which we are aware. It is evident that Wannier interpolation combined with adaptive smearing enables highly accurate DOSs, allowing even the very finest of features to be captured. As we would expect, there is a dramatic increase in the DOS at the Fermi level as the pressure is increased through the A7 → sc phase transition, during which arsenic changes from a semimetal to a metal. We have used our DOS calculations to recompute the Fermi energy of A7 arsenic at 0 GPa. We obtain a value that is 0.01 eV higher than that resulting from our self-consistent calculation using the PWSCF code, moving the Fermi level toward the minimum in the DOS that appears nearby.

Next we inspect the evolution of the DOS of arsenic in the immediate vicinity of the A7 → sc transition, and present our results in Fig. 8. In this figure, the DOSs for arsenic at 29 and 25 GPa are referenced to the Fermi level and superimposed. Changes in the DOS are observed more clearly as the pressure is lowered such that arsenic transitions from the higher-symmetry sc phase to the lower-symmetry A7 phase (the sc → A7 transition). Thus we see from this figure that the onset of the Peierls-type cubic to rhombohedral distortion is signified by the emergence of van Hove singularities in the DOS, especially around the Fermi level. The rapidly changing

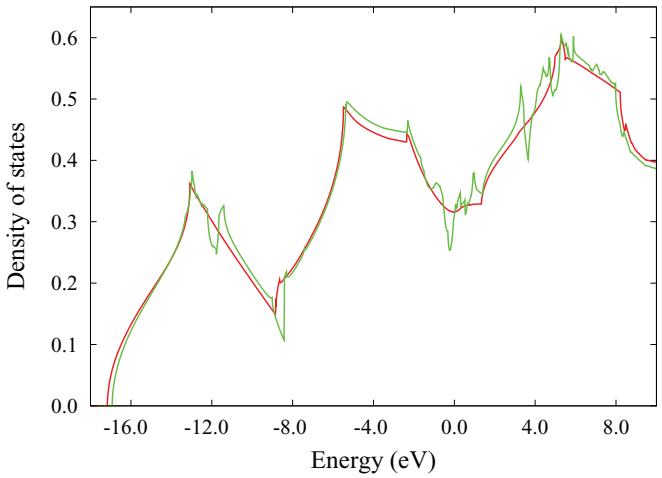

FIG. 8. (Color online) Evolution of the DOS of arsenic across the sc → A7 phase transition. The DOSs of arsenic at 29 (black/red) and at 25 GPa (gray/green) are referenced to the Fermi level and superimposed. It can be seen that as the pressure is lowered, the onset of the Peierls-type cubic to rhombohedral distortion is signified by the emergence of van Hove singularities in the DOS.

DOS at the Fermi level explains why such high levels of convergence are required when studying this transition.[10]

In our earlier studies of arsenic,[10] we had found that the rhombohedral angle α reaches its high-symmetry value at a lower pressure than does the atomic positional parameter z, and that the electronic change occurring as the pressure is increased through the A7 → sc transition appeared to be driving the atomic positional parameter z to its high-symmetry value. A close inspection of the evolving DOS however, which can be seen in the Supplemental Material,[16] reveals that the electronic change is instead driving α to its high-symmetry value.

VII. CONCLUSIONS

Wannier interpolation has enabled us to calculate the Fermi surface of arsenic at ambient pressures and through the A7 → sc phase transition, obtaining first-principles accuracy at vastly reduced computational cost. We found that the folding of the Fermi surfaces is perhaps the best indication of when the A7 → sc phase transition has occurred. We further determined from our studies of the Wannier-interpolated DOS of arsenic over the range of pressures in the vicinity of the A7 → sc phase transition, that the onset of the Peierls-type cubic to rhombohedral distortion is signified by the appearance of emerging van Hove singularities in the DOS especially around the Fermi level. The rapidly changing DOS at the Fermi level explains why such high levels of convergence are required when studying this transition, as we had found in our earlier studies of arsenic.[10]

Arsenic provides us with an example of a challenging system that is ideally suited to demonstrating the power of the Wannier interpolation technique. This methodology furthermore enables a novel approach to the study of semimetal to metal phase transitions, such as the A7 → sc transition of arsenic, or in fact of any phase transitions involving a metal. The technique is a particularly valuable one for the accurate determination of Fermi surfaces, as well as for the calculation of highly resolved DOSs.

ACKNOWLEDGMENTS

We thank Richard Needs for helpful discussions. Computing resources were provided by the University of Cambridge High Performance Computing Service (HPCS). P.D.H. and J.R.Y. acknowledge the support of Royal Society University Research Fellowships.

[1] O. Degtyareva, M. I. McMahon, and R. J. Nelmes, High Press. Res. **24**, 319 (2004).
[2] P. J. Lin and L. M. Falicov, Phys. Rev. **142**, 441 (1966).
[3] J. R. Yates, X. Wang, D. Vanderbilt, and I. Souza, Phys. Rev. B **75**, 195121 (2007).
[4] X. Wang, J. R. Yates, I. Souza, and D. Vanderbilt, Phys. Rev. B **74**, 195118 (2006).
[5] X. Wang, D. Vanderbilt, J. R. Yates, and I. Souza, Phys. Rev. B **76**, 195109 (2007).
[6] F. Giustino, J. R. Yates, I. Souza, M. L. Cohen, and S. G. Louie, Phys. Rev. Lett. **98**, 047005 (2007).
[7] N. Marzari and D. Vanderbilt, Phys. Rev. B **56**, 12847 (1997).
[8] I. Souza, N. Marzari, and D. Vanderbilt, Phys. Rev. B **65**, 035109 (2001).
[9] N. Marzari, A. A. Mostofi, J. R. Yates, I. Souza, and D. Vanderbilt, Rev. Mod. Phys. **84**, 1419 (2012).
[10] P. Silas, J. R. Yates, and P. D. Haynes, Phys. Rev. B **78**, 174101 (2008).
[11] H. J. Beister, K. Strössner, and K. Syassen, Phys. Rev. B **41**, 5535 (1990).
[12] T. Kikegawa and H. Iwasaki, J. Phys. Soc. Jpn. **56**, 3417 (1987).
[13] See the Supplemental Material of Ref. 10, available at http://link.aps.org/supplemental/10.1103/PhysRevB.78.174101 for the convergence properties of the A7 → sc phase transition.
[14] G. H. Wannier, Phys. Rev. **52**, 191 (1937).
[15] N. Marzari, D. Vanderbilt, A. De Vita, and M. C. Payne, Phys. Rev. Lett. **82**, 3296 (1999).
[16] See Supplemental Material at http://link.aps.org/supplemental/10.1103/PhysRevB.88.134103 for the following: a review of the BZ of the two-atom primitive cell of A7 arsenic; a discussion concerning the choice of the number of Wannier functions to construct in order to set up an "exact tight-binding" model of the system at each given pressure, from which Wannier interpolations can be performed; an elaboration on the features of the electron and hole Fermi surfaces of A7 arsenic at 0 GPa; an investigation of sc arsenic at 35 GPa using the one-atom primitive cell to inspect the "unfolded" Fermi surfaces, and to compare with the folded ones resulting from the use of the two-atom unit cell; results of our studies of arsenic at pressures beyond which it is no longer in the sc phase (once again using the two-atom unit cell); an elaboration on our studies of the DOS of arsenic as it undergoes the A7 → sc phase transition, and DOSs and corresponding band structures for A7, sc, and body-centered-cubic (bcc) arsenic; and various animations

created to illustrate the evolution of the Fermi surface of arsenic across the A7 → sc transition.

[17]P. Giannozzi, S. Baroni, N. Bonini, M. Calandra, R. Car, C. Cavazzoni, D. Ceresoli, G. L. Chiarotti, M. Cococcioni, I. Dabo *et al.*, J. Phys.: Condens. Matter **21**, 395502 (2009).

[18]A. A. Mostofi, J. R. Yates, Y.-S. Lee, I. Souza, D. Vanderbilt, and N. Marzari, Comput. Phys. Commun. **178**, 685 (2008).

[19]J. P. Perdew, K. Burke, and M. Ernzerhof, Phys. Rev. Lett. **77**, 3865 (1996).

[20]G. S. Cooper and A. W. Lawson, Phys. Rev. B **4**, 3261 (1971).

[21]M. H. Cohen, Phys. Rev. **121**, 387 (1961).

[22]L. M. Falicov and S. Golin, Phys. Rev. **137**, A871 (1965).

[23]A. Kokalj, Comput. Mater. Sci. **28**, 155 (2003).

[24]L. M. Falicov and P. J. Lin, Phys. Rev. **141**, 562 (1966).

[25]M. G. Priestley, L. R. Windmiller, J. B. Ketterson, and Y. Eckstein, Phys. Rev. **154**, 671 (1967).

[26]L. R. Windmiller, Phys. Rev. **149**, 472 (1966).

[27]C. S. Ih and D. N. Langenberg, Phys. Rev. B **1**, 1425 (1970).

[28]Thus far, our Fermi energies have been obtained using the PWSCF code.[17] Unless otherwise indicated, our depictions of the Fermi surface of arsenic have also been obtained using these values. Our measurements of the cross sections of the Fermi surface of arsenic at 0 GPa, however, have been calculated using a more precise value of the Fermi energy, recomputed from a Wannier-interpolated DOS we present in Sec. VI.

[29]M. H. Cohen, L. M. Falicov, and S. Golin, IBM J. Res. Dev. **8**, 215 (1964).

[30]R. M. Martin, *Electronic Structure: Basic Theory and Practical Methods* (Cambridge University Press, Cambridge, 2004).

[31]L. F. Mattheiss, D. R. Hamann, and W. Weber, Phys. Rev. B **34**, 2190 (1986).